Metastable Precursor Structures in Hydrogen-infused Super Duplex Stainless Steel Microstructure – An Operando Diffraction Experiment

DOI:
10.1016/j.corsci.2020.109021

Corrosion Science 176 (2020) 109021

Contents lists available at ScienceDirect

Corrosion Science

journal homepage: www.elsevier.com/locate/corsci

Metastable precursor structures in hydrogen-infused super duplex stainless steel microstructure – An operando diffraction experiment

Cem Örnek [a,*], Alfred Larsson [b], Gary S Harlow [c], Fan Zhang [d], Robin Kroll [e], Franceso Carlà [f], Hadeel Hussain [g], Ulf Kivisäkk [g], Dirk L Engelberg [e], Edvin Lundgren [b], Jinshan Pan [d,*]

[a] Istanbul Technical University, Department of Metallurgical and Materials Engineering, Istanbul, Turkey
[b] Lund University, Division of Synchrotron Radiation Research, Lund, Sweden
[c] Department of Chemistry, Nano-Science Center, University of Copenhagen, Copenhagen, Denmark
[d] KTH Royal Institute of Technology, Division of Surface and Corrosion Science, Stockholm, Sweden
[e] University of Manchester, Department of Materials, Materials Performance Centre, Manchester, United Kingdom
[f] Diamond Light Source, Didcot, United Kingdom
[g] Sandvik Materials Technology, Sandviken, Sweden

ARTICLE INFO

Keywords:
Grazing-incidence x-ray diffraction (GIXRD)
Synchrotron radiation
Duplex stainless steels
Hydride
Hydrogen embrittlement

ABSTRACT

We report the evolution of metastable precursor structures during hydrogen infusion in the near-surface region of a super duplex stainless steel. Grazing-incidence x-ray diffraction was employed to monitor, operando, the lattice degradation of the austenite and ferrite phases. Electrochemical hydrogen charging resulted in the splitting of the diffraction peaks of the austenite phase, suggesting the evolution of a metastable precursor structure. This may be explained by the formation of quasi-hydrides, which convert back into the austenite parent structure during hydrogen effusion. The ferrite showed less lattice deformation than the austenite and no phase transformation.

1. Introduction

Super duplex stainless steels (SDSSs) are work-horse materials and are generally used in demanding engineering applications due to their high strength and superior resistance to corrosion and hydrogen-induced material degradation compared to various counterpart single-phase stainless steels [1,2]. However, several failures of offshore components, subjected to cathodic hydrogen exposure for several years (cathodic protection), have been reported [3,4]. These materials had a very coarse microstructure with a grain size in the order of >50 μm on average [3,4] or were cold-worked [5]. In contrast, no failure due to hydrogen embrittlement has been reported for SDSSs with finely-grained solution-annealed microstructures with an austenite spacing of less than 10 μm [1]. Earlier research has pointed out that finely-grained duplex microstructures are significantly less sensitive to hydrogen-induced degradation [1,6]. Therefore, we need to understand the reasons for a possible immunity of finely-grained SDSSs to hydrogen embrittlement in application-relevant conditions. Grain boundaries, in particular phase boundaries, in duplex microstructures serve as trap sites for hydrogen, which reduce the susceptibility to hydrogen-induced cracking. Trapped hydrogen in steels has been reported to be innocuous, and only mobile hydrogen in the microstructure causes embrittlement [7].

Characterization of the effect of hydrogen in microstructures is challenging as it requires real-time measurements with a high spatial and temporal resolution [8–10]. This problem necessitates access to large-scale research facilities. Earlier work indicated that hydrogen embrittlement might consist of metastable degradation events that are only accessible if measured with high temporal resolution and sufficient sensitivity [6,11,12]. It has been shown that hydrogen interacts more with the austenite than ferrite in duplex stainless steel microstructures [13]. Hydrogen infusion into the austenite resulted in the formation of tensile strains that were significantly higher than those developed in the ferrite. In parallel, the ferrite was seen to undergo compression along the tensile loading direction [13]. The austenite phase typically dissolves more hydrogen than the ferrite phase, but the hydrogen in the ferrite phase is able to diffuse with orders of magnitude faster rates than in the austenite [7,14,15]. These, hence, ultimately result in the localization of

* Corresponding author.
E-mail addresses: cornek@itu.edu.tr (C. Örnek), alfred.larsson@sljus.lu.se (A. Larsson), gary.harlow@chem.ku.dk (G.S. Harlow), fanzhang@kth.se (F. Zhang), robin.kroll@postgrad.manchester.ac.uk (R. Kroll), francesco.carla@diamond.ac.uk (F. Carlà), hadeel.hussain@diamond.ac.uk (H. Hussain), ulf.kivisakk@sandvik.com (U. Kivisäkk), dirk.engelberg@manchester.ac.uk (D.L. Engelberg), edvin.lundgren@sljus.lu.se (E. Lundgren), jinshanp@kth.se (J. Pan).

https://doi.org/10.1016/j.corsci.2020.109021
Received 5 June 2020; Received in revised form 15 September 2020; Accepted 18 September 2020
Available online 23 September 2020

hydrogen and a time-dependent evolution of lattice changes in the microstructure.

The objective of this work is to reveal metastable activities or reversible processes associated with hydrogen infusion, that are accessible if measured in-situ and in real-time only, and to understand the earliest stages of material degradation induced by the interaction of hydrogen with the microstructure. Synchrotron grazing-incidence x-ray diffraction (GIXRD) was employed to observe, operando, the lattice changes in the austenite and ferrite phases during electrochemical hydrogen charging to gain insight into hydrogen-microstructure interactions. This work provides high temporal resolution and detection sensitivity to structural changes occurring during hydrogen infusion into stainless steel microstructure.

2. Experimental

The material used was a commercial-grade SAF 2507 SDSS with a finely-grained microstructure, supplied by Sandvik Materials Technology, Sweden. The investigated microstructure had a ferrite and austenite grain size of 5−10 μm, with an austenite spacing of 4 μm. The microstructure of the investigated SDSS is shown in Fig. 1, highlighting the spatial distribution and connectivity of both phases. Samples were cut from a tube material, with the surface pointing outward to the tube diameter. The specimens were successively ground to 4000-grit (EU grade) size using SiC sandpapers, followed by polishing down to ¼ μm, to achieve a mirror-finish surface. The chemical composition (in wt.-%) was 25.35 % Cr, 6.46 % Ni, 3.85 % Mo, 0.44 % Mn, 0.28 % Si, 0.13 % Cu, 0.29 % N, and other trace elements.

An electrochemical cell was 3D-printed to expose the specimens to an electrolyte while applying a cathodic current/potential to charge the specimens with hydrogen. The cell walls were made of a PEEK foil with 100 μm thickness that was amorphous and translucent to high-energy x-rays. The specimen, together with a platinum-wire counter electrode, and a miniature-sized Ag/AgCl (sat.) reference electrode was mounted into the cell and sealed with ultra-fast drying silicone. The cell had inlet and outlet ports to continuously pump the solution, using a peristaltic pump, to remove bubbles generated during electrochemical charging and to provide fresh electrolyte into the system. A Gamry Reference 600+ potentiostat was used to control the applied current and potential.

Synchrotron GIXRD measurements were carried out to reveal lattice changes occurring in the near-surface region with a probing depth of approximately 170 nm, determined according to Welzel et al. [16]. The surface is the place where the first contact with hydrogen occurs, and the location where most and first material degradation happens. Therefore, the aim was to understand the most incipient stages of hydrogen-induced degradation of SDSS. The GIXRD measurements were conducted at the beamline I07 at Diamond Light Source in the UK. The energy of the x-rays was 20.5 keV with a beam size of 100 μm (vertical) x 300 μm (horizontal) at the sample position. The experiment was performed with a DECTRIS Pilatus 100 K two-dimensional detector with an area of 487×195 pixels (each $172 \times 172\ \mu m^2$) mounted on the diffractometer arm at a distance of 900 mm from the sample. The near-surface was probed with an incidence angle of 0.2°; thus, the projected x-ray beam onto the surface was 300 μm x 500 μm, producing diffraction signals from approximately 100–300 grains. At the same time, the sample was subjected to static cathodic hydrogen charging in 1 M NaCl at room temperature. The electrochemical cell used for hydrogen charging and the diffraction measurement setup is schematically illustrated in Fig. 2.

Diffraction measurements were first carried out under potentiostatic control at −1500 mV (vs. Ag/AgCl) to simulate near-realistic conditions (the cathodic protection potential is between −1050 and −1150 mV vs. Ag/AgCl [1]), but also to accelerate the absorption of hydrogen into the microstructure. The diffraction patterns were measured out-of-plane (along the specular direction) with an angular range of 2.3° 2θ on the detector. This setup provides information about strain evolution in the direction perpendicular to the surface with a deviation of half the Bragg angle minus the grazing angle (0.2°), which results in 8.2° for the austenite phase and 8.5° for the ferrite phase. The diffraction signals were collected by moving the detector while maintaining a fixed sample position. The 2θ range for the diffraction measurement was 15.8–36.1°, capturing signals from five Bragg peaks for the austenite and three peaks from the ferrite (Fig. 2).

The second set of experiments focused on time-lapse diffraction measurements under galvanostatic control with a current density of $-37.5\ mA/cm^2$ at the angular range 15.5–17.8° 2θ. These experiments were designed to monitor the reflection of the austenite phase with 111 orientation and the ferrite phase with 110 orientation with higher temporal resolution (2.9 s/frame). The specimen was subjected to galvanostatic hydrogen absorption for 1760 s. Then, the charging was stopped, and the diffraction measurements were continued for 940 s to measure hydrogen desorption (effusion), giving a total measurement time of 2700 s. Hence, it was possible to measure the lattice changes during hydrogen absorption (infusion) and desorption under operando conditions. The penetration depth of hydrogen at room temperature in ferrite and austenite was estimated from the diffusion coefficients provided by Mente and Boellinghaus [17], which was 7.7 μm/s for the ferrite and 24 nm/sec for the austenite. Thus, 1760 s of hydrogen charging resulted in minimum penetration depth of 4.2 μm in austenitic grains, and the ferrite grains were infused to the center of the specimen.

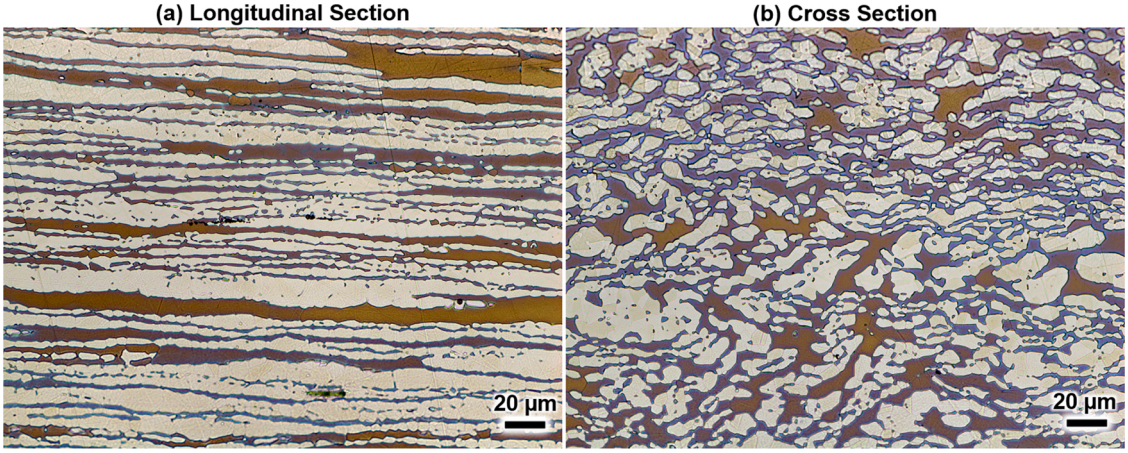

Fig. 1. Optical micrographs after electrochemical etching using 40 wt.-% KOH solution showing the microstructure of the investigated SDSS. The ferrite is the matrix phase shown as brown color whereas the austenite is embedded in the ferrite shown with white contrast (Note: only the distributions of both crystallographic phases is shown here and not the grain sizes).

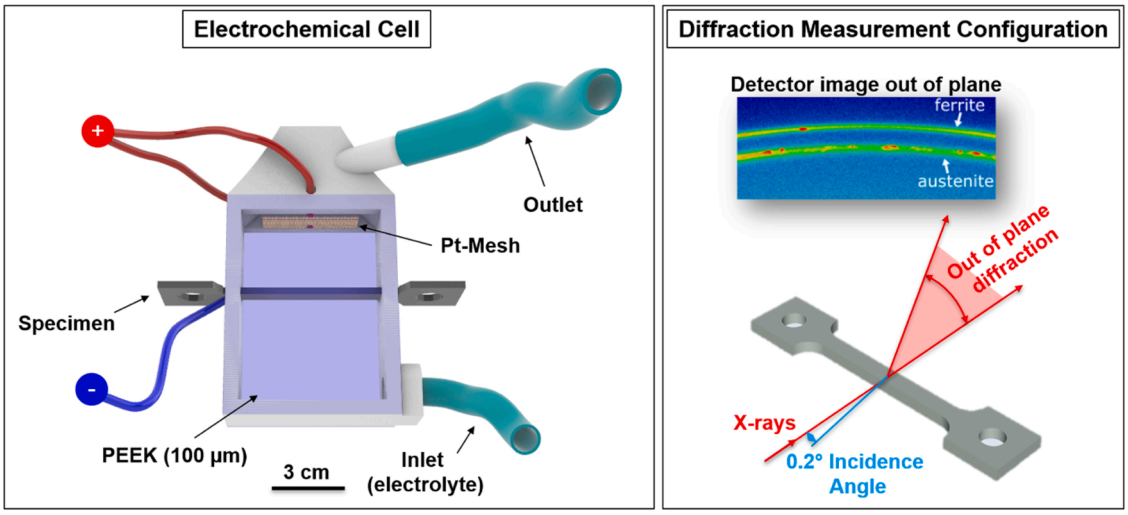

Fig. 2. (Left) The electrochemical cell used for hydrogen charging. The frame of the cell was made of 3D-printed polylactic acid. (Right) GIXRD measurement configuration showing out-of-plane 2D-diffraction patterns.

The surface grains of the austenite phase became nearly saturated with hydrogen during the charging experiment.

All 2D-diffraction data were converted into 1D patterns, as described elsewhere [18], and details about the experimental method can be found in earlier published work [19]. The 1D-diffraction peaks were fitted using the Gaussian_LorenCross (a mixture of Gaussian and Lorentzian line shapes) fitting function in OriginLab V2020b to determine the peak positions. This fitting function gave the best results among all common fitting functions. The change in peak position versus the uncharged position was calculated and denoted as macrostrain, as described elsewhere [20,21]. The reported strains do not reflect the absolute strain states in the microstructure and provide only relative changes that occurred due to hydrogen interaction with the lattice.

3. Results and discussion

The operando diffraction results of the specimen subjected to potentiostatic hydrogen charging at −1500 mV are summarized in Fig. 3. The absorption of hydrogen resulted in large lattice deformation, with the austenite phase undergoing more severe deformation than the ferrite. The evolution of the strains in the austenite perpendicular to the surface was tensile, which means that the lattice expanded along with that direction. It should be noted that we report only relative strains with reference to the uncharged condition. The microstructure of duplex stainless steel typically has residual strains which may vary over the position in the specimen in all directions. So, the evolution of tensile strain may not mean that the austenite is under tension since compressive strains may have been operating. However, the development of tensile stresses indicates that the magnitude of compressive forces, if any, is reduced.

The diffraction peaks both altered in shape and position, indicating the evolution of micro- and macro-deformation. Micro-strains are the deformation that occur on a grain scale (intra-granular), whereas macro-strains are those that operate over a broader range of grains (inter-granular and all grains) [22]. The positional changes of a diffraction peak, however, may also be caused by chemical alterations, which typically are more substantial than those caused by deformation. The infusion of hydrogen in our experiment was chemical alloying; therefore, severe shifts of the diffraction peaks of the austenite phase were observed. The austenite can dissolve an order of magnitude more hydrogen atoms than the ferrite [7,23,24], which explains the reason for the shifts. However, chemical effects are also reflected by an instantaneous deformation of the lattice as it becomes distorted by the hydrogen, but a deconvolution of chemical forces and strain is not trivial. Nevertheless, the results indicated that the most significant contribution to the peak shift was due to the entered hydrogen into the lattice as, during desorption, most of the macro-strains reverted, showing elastic deformation to have occurred.

Moreover, the austenite peak intensity was significantly reduced, with the development of a discrete second peak (a separate diffraction spot on the 2D image captured) close to the austenite peaks via peak splitting, as seen in Fig. 3a-c. A more detailed investigation was conducted on the 2-Theta region shown in Fig. 3b, encompassing the 111-austenite and 110-ferrite Bragg peaks, to investigate the observed peak splitting further. Time-lapse diffraction measurements of the 111-austenite peak during hydrogen charging and discharging showed that the nature of the peak splitting had a metastable character, as the new peaks reverted to austenite during the discharging cycle, summarized in Fig. 4. The results of the operando GIXRD experiments during galvanostatic hydrogen charging are also presented in Video 1. Fig. 4 shows three frames from Video 1 at different times. The absorption of hydrogen shifted the positions of the austenite and ferrite peaks to lower 2-Theta values indicating lattice expansion, with the austenite changing more than the ferrite. The absorption of hydrogen led to the evolution of a diffraction peak in proximity to the 111-austenite diffraction peak within a few seconds of charging. The intensity of the austenite peak decreased when the new peak position developed, indicating a heterogeneous lattice deformation of the austenite that is associated with the evolution of a new precursor structure that potentially precedes crack evolution. This observation suggests that near-surface austenite grains became rapidly saturated with dissolved hydrogen that resulted in peak splitting.

The peak splitting occurred on individual grains only (Fig. 4), pointing toward a higher propensity of certain grains to hydrogen-induced structural modification of the lattice. The 110-peak of the ferrite did not show peak splitting. The ferrite peak intensity did not change during hydrogen charging and discharging. Our experiments have shown that the uptake of hydrogen and its interaction with the microstructure is heterogeneous and dynamic. This has shown that the austenite is the load-bearing phase, supporting the ferrite in maintaining the structural integrity of the microstructure of duplex stainless steel. Most hydrogen and strain are accommodated by the austenite reducing thereby the load-burden on the ferrite phase, supporting increased resistance to hydrogen embrittlement. The new peaks disappeared upon the termination of the hydrogen charging, indicating that the process is reversible.

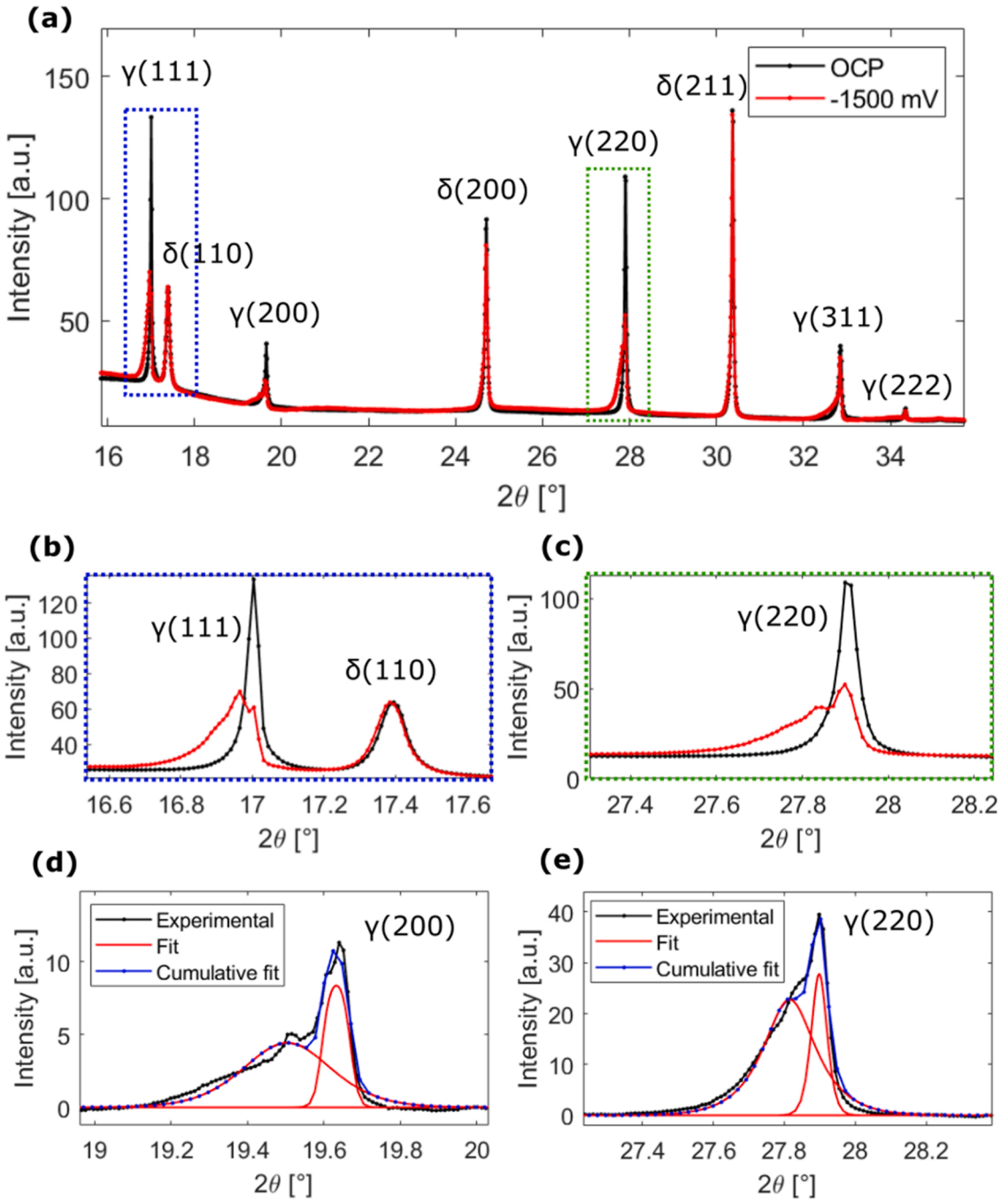

Fig. 3. Operando GIXRD measurement results obtained during electrochemical hydrogen charging under potentiostatic control at −1500 mV vs. Ag/AgCl (sat.): (a) showing the main reflections of the austenite and ferrite phases, (b) showing the 111-peak of the austenite and 110-peak of the ferrite with a magnified view, and (c) showing the 220-reflection of the austenite with a magnified view, (d-e) showing the diffraction peaks for 200 and 220 austenite with fitting results.

However, no additional diffraction rings other than that of the parent phases were present, which might suggest that no new phase had formed. However, the observed peak splitting may be a precursor stage of the formation of possible hydrides that have been documented in austenitic stainless steel [25,26]. It has been reported that when the hydrogen in the lattice reaches a threshold concentration, hydrides, having a crystallographic orientation relationship with the host lattice, can be formed [10,25–27]. $FeH_{0.13}$ and NiH_x ($x \leq 1.25$) type of hydrides with face-centered-cubic (fcc) structure have been observed under electrolytic charging conditions [27]. Kamachi [26] and Chen et al. [25] reported hydrides that formed in different types of austenitic stainless steels under electrochemical charging. Two different types of hydrides were formed; one was having a face-centered cubic structure with a slightly larger lattice constant and another with hexagonal closely-packed lattice [25,26]. There is an agreement that the hydrides are metastable at room temperature and that they transform rapidly back to austenite [25,26]. However, phase identification requires chemical evidence, which was not reported by Kamachi [26] and Chen et al. [25]. Chemical detection of hydrogen in a compound is, however, not trivial, and via x-ray experiments, hydrogen cannot be detected directly.

Our experimental data clearly showed that a change in the atomic structure occurs during cathodic hydrogen charging, and disappears when hydrogen desorbs, indicating a metastable character that cannot

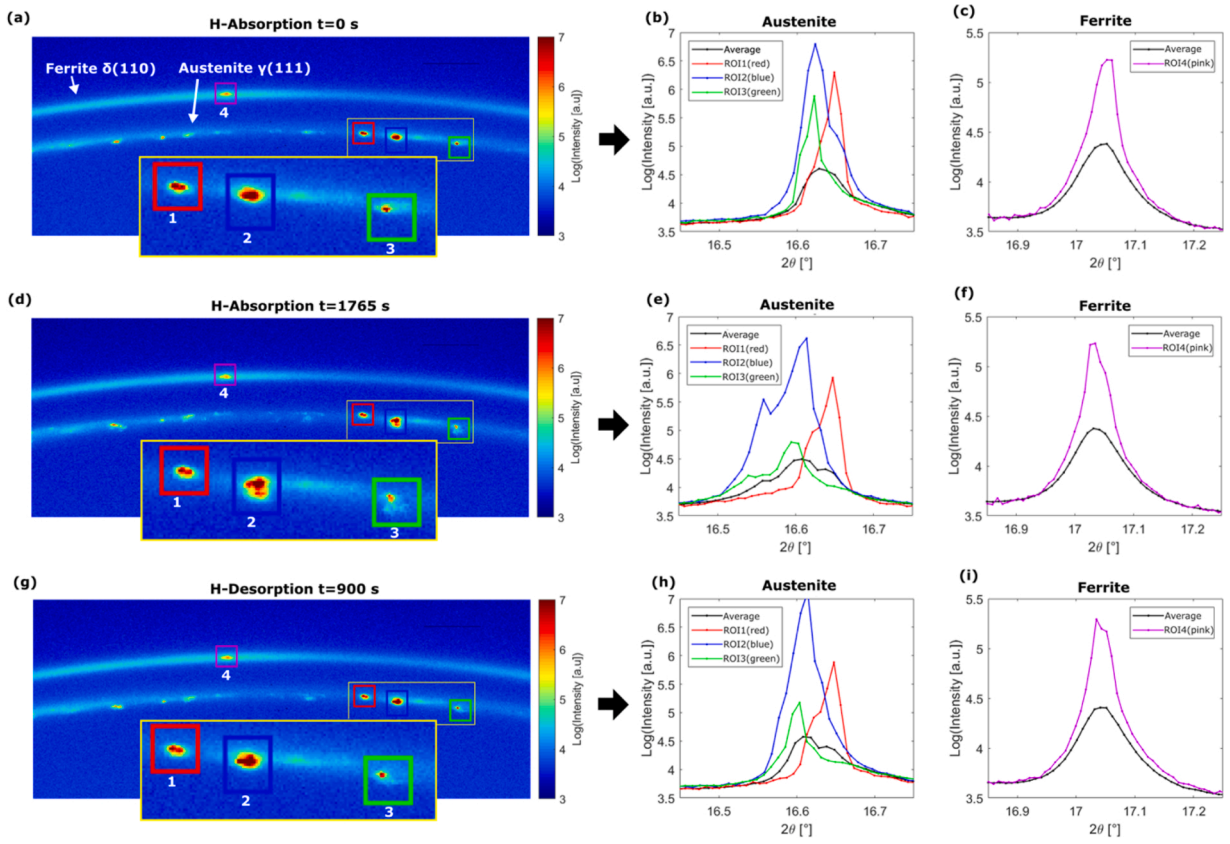

Fig. 4. Snapshots from the operando, real-time GIXRD measurements during galvanostatic hydrogen charging with a current density of −37.5 mA/cm^2. The 2D-diffraction images on the left show the diffraction signals from the austenite (111) and ferrite (110) phase. The graphs on the right-hand side are data extracted from partial integration over the highlighted regions in the diffraction images. (a-c) show diffraction information at t = 0 s (uncharged condition), (d-f) show the diffraction data for hydrogen charging at 1765 s, (g-i) show the real-time diffraction data 900 s after the termination of hydrogen charging (1800 s). The average diffraction peak is from the entire azimuthal projection in the 2D-diffraction image.

be explained by the evolution of strains only. The average strain formation due to hydrogen infusion in the austenite phase by considering the peak shift of the main diffraction peak was $2{\cdot}10^{-3}$. This already indicates plastic deformation. When, however, the position of the new diffraction peak is considered for macrostrain evolution, then the maximum strains become $6{\cdot}10^{-3}$, which would indicate three times higher deformation. Such large deformation would produce a residual change to the lattice; however, the experimental results clearly showed that most of the lattice change is reversible, indicating that more than simple elastic deformation should be considered. Hence, this suggests that a new chemical phase was formed during the time of charging.

The new phase has a structure very similar to that of the host lattice, and the diffraction peak intensity of the host lattice decreased with time, while that of the new structure increased, indicating the conservation of material. This suggests that the new structure transforms by the conversion of the host austenitic lattice. It seems that the structure forms at individual grains only or more preferentially (see ROI 2 and ROI 3 in Fig. 4). We have conducted additional operando diffraction experiments at more negative electrode potentials (up to -1.9 V) and have seen that the peak splitting becomes more pronounced, resulting in distinctive peak separation (data not shown). We have further conducted simple ab-initio first-principles calculation based on density-functional theory (DFT)[1] to see whether hydrides can be formed. The DFT calculation results revealed that hydride formation is possible in the studied duplex stainless steel, with NiH providing the most energetically favored hydride as contrasted to CrH, Cr_2H, and FeH. The formation energy of NiH is exothermic (−112 mV), which forms a face-centered-cubic (fcc) lattice with only a few percent larger cell structure than the host lattice. Other possible exothermic hydrides were FeH, CrH, and Cr_2H, which have exothermic formation energy of −56 mV, −45 mV, and −30 mV, respectively, but these are less likely as nickel forms stronger hydrides. The diffraction patterns of the possible hydrides were simulated, and the closest peak position to the newly formed peak was seen to be the peaks of NiH. However, as the data shows, the peak splitting is not an instantaneous event of the formation of a fixed-determined chemistry and lattice structure, but rather is a process that lasted throughout the charging period, showing gradual accumulation and evolution. So, the new structure may not be a true hydride with fixed composition and lattice structure but instead seems to be a quasi-hydride that is a hydrogen-rich austenitic lattice.

The observed peak splitting cannot be associated with any kind of martensite (α' or ε) formation as the positions of the detected peaks do not indicate any other lattice structure than face-centered cubic. Martensite can be formed in austenitic stainless steel [28] or transformation-induced plasticity duplex stainless steel [29] and is typically formed due to large strains. However, martensite formation in SDSS is not favored due to the presence of nitrogen in high concentrations. Strain-induced martensite has not been reported, to our knowledge, in SDSS with high nitrogen content. Strain-induced martensite has been observed in grade 22Cr-5Ni duplex stainless steel but only at very high levels of plastic deformation [30]. However, no hydrogen-induced martensite was observed when the same duplex material was subjected to cathodic hydrogen charging [30]. In our work, the material was not subjected to any mechanical load but only to hydrogen absorption. So,

[1] The DFT calculation was done on https://materialsproject.org/ by searching for hydrides of Fe, Cr, and Ni.

the observed peak splitting is therefore unlikely to be due to any kind of martensite formation.

The local concentration of hydrogen in the austenite can reach higher values than in the ferrite due to higher solubility and lower diffusion kinetics of atomic hydrogen [7–9,31]. Therefore, structural changes are more likely to occur in the austenite in duplex stainless steel microstructures. So, the reason for the peak splitting can only be due to large but highly heterogeneous lattice expansion of austenite grains, suggesting quasi-hydrides to have formed. Therefore, we believe that peak splitting is a positive response (i.e., mitigating hydrogen embrittlement) of the microstructure regarding hydrogen-induced lattice degradation. Coarsely-grained microstructures cannot accommodate a large amount of hydrogen that ultimately results in cracking. In contrast, microstructures with smaller grain sizes can immobilize the hydrogen by trapping and/or formation of quasi-hydrides. As the whole process is reversible, the microstructure with small austenite spacing can accommodate more (elastic) strain (and hydrogen) and is, therefore, more resistant to hydrogen embrittlement. The quasi-hydrides are not stable and revert back once cathodic charging has ceased. It should be further noted that the evolution of these quasi hydrides may not be an adverse effect regarding to hydrogen embrittlement. The austenite could accommodate three-times more macro-deformation due to the presence of the quasi hydrides, which in turn was beneficial to the entire duplex microstructure as no surface cracks were observed upon termination of the charging experiments.

The saturation of near-grain boundary regions of large grains can lead to high lattice deformation compared to areas with less hydrogen. The high deformation is, interestingly, mostly elastic. Smaller grains become saturated faster than larger ones, with the grain orientation possibly also having an influence. Hence, more significant hydrogen-induced strain gradients may develop across larger grains. This may explain the reason for more substantial lattice strain evolution observed on individual grains, as apparent from discrete 2D diffraction intensities (Fig. 4). The increase in deformation is associated with the generation of defects in the microstructure, which leads to more hydrogen uptake and hence resulting in a higher concentration of dissolved hydrogen. Linear defects can line up and form sub-grain boundaries that can further increase H uptake. Larger grains can then develop higher partial pressures than smaller ones, suggesting more deformation. This, in turn, may explain the reason for the superior resistance of super duplex stainless steel with small austenite spacing (equivalent to small grains) to hydrogen embrittlement as compared to coarsely-grained microstructures. It should be noted that such a large peak shift should have resulted in plastic macro-deformation. However, the peak splitting was reversible and showed that most the strain was elastic. Elastic strain theory cannot explain the large shifts; therefore, this argument corroborates the evolution of a quasi-hydrides, well-likely a form of NiH. The hydrides observed by Kamachi [26] and Chen et al. [25] were stable at room temperature, but these were seen in austenitic stainless steel that contained 18 wt.-% Ni. We believe the nickel (content) plays a crucial role in the evolution of hydrides. Hydride formation may not be a negative, unwanted occurrence regarding hydrogen embrittlement. The development of hydride shows that the microstructure can accommodate large amounts of hydrogen and immobilize it, as contrasted to the ferrite that is susceptible to hydrogen-induced cracking. So, the evolution of quasi-hydrides in super duplex stainless steel may explain the reason why finely-grained microstructures have superior resistance to hydrogen embrittlement than coarsely-grained microstructures, as the latter showed less or no peak splitting.

The strain evolution of individual regions of the austenite and ferrite was analyzed in more detail in Fig. 5. The integration over the entire portion of the 2D-diffraction ring did not show peak splitting (average 1D-pattern in Fig. 5). There are some individual grains that were more affected than others. The diffraction data suggest that the ferrite underwent a more homogeneous deformation as no discrete changes in the 2D-diffraction pattern were seen. It is propitious that the austenite

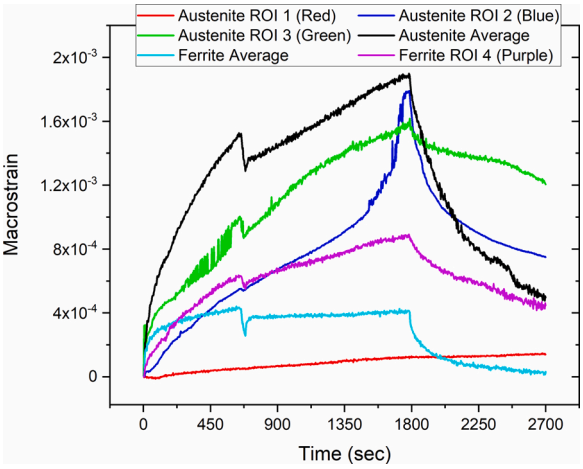

Fig. 5. Determination of the macrostrains of selected regions, as highlighted in Fig. 4 and Video 1. The strain evolution of selected austenitic and ferritic regions. The direction of the strain evolution is approximately perpendicular to the surface of the specimen.

accommodates most hydrogen and deformation, protecting thereby the ferrite. The austenite is the far more ductile phase and less susceptible to cracking reasoned by dissolved hydrogen.

Implications – Our work has shown that metastable structures can be formed during electrochemical hydrogen charging without the need for external stresses. These were formed in the austenite phase, which showed higher lattice deformation than the ferrite phase. This observation indicates that in the duplex stainless steel microstructure, the behavior of the austenite phase primarily matters regarding hydrogen embrittlement. The ferrite phase is often considered responsible for hydrogen embrittlement since cracks have frequently been observed to initiate at and propagate through ferritic grains, with the austenite grains typically having an effect on crack deflection or arrest [3,4,32–36]. Those observations, however, were made on coarsely-grained microstructures with austenite spacing >30 µm or cold-worked materials. The results of our work suggest that the austenite (in finely-grained microstructure) can accommodate high concentrations of hydrogen and severe deformation without transmitting a high mechanical burden on ferritic grains. It seems that as long as the austenite phase has a high accommodation capacity for hydrogen and lattice strain, the ferrite phase is protected from hydrogen embrittlement. No sign of any cracking was seen on austenite and ferrite grains when imaged in a scanning electron microscope after the termination of our experiments. This demonstrates the superior resistance to hydrogen embrittlement of the austenite phase despite the more interaction (deformation) with hydrogen occurred.

4. Conclusions

- Electrochemical hydrogen charging led to the evolution of heterogeneous tensile lattice strains predominantly occurring in the austenite phase.
- The infusion of hydrogen led to splitting of the diffraction peaks of the austenite phase, which reverted rapidly back to austenite during the effusion of hydrogen.
- The observation of the peak splitting points towards the formation of a precursor structure, suggesting the evolution of a metastable hydride.
- Hydrogen-induced lattice strain formation is reversible, with the earliest onset of hydrogen embrittlement associated with the degradation of the austenite phase.

- The austenite phase supports and probably protects the ferrite phase by mostly accommodating infusing hydrogen into the duplex stainless steel microstructure.

Data availability statement

The raw/processed data required to reproduce these findings will be shared by the corresponding author upon reasonable request.

CRediT authorship contribution statement

Cem Örnek: Conceptualization, Methodology, Software, Formal analysis, Investigation, Visualization, Data curation, Writing - original draft, Writing - review & editing, Project administration, Funding acquisition. **Alfred Larsson:** Software, Formal analysis, Investigation, Data curation, Writing - review & editing, Visualization. **Gary S Harlow:** Software, Formal analysis, Investigation, Writing - review & editing. **Fan Zhang:** Investigation, Software, Writing - review & editing. **Robin Kroll:** Investigation, Software, Writing - review & editing. **Franceso Carlà:** Methodology, Software, Investigation, Resources, Writing - review & editing. **Hadeel Hussain:** Investigation, Resources, Writing - review & editing. **Ulf Kivisäkk:** Conceptualization, Methodology, Resources, Writing - review & editing. **Dirk L Engelberg:** Conceptualization, Methodology, Investigation, Writing - review & editing, Supervision, Funding acquisition. **Edvin Lundgren:** Methodology, Writing - review & editing, Supervision, Funding acquisition. **Jinshan Pan:** Conceptualization, Methodology, Formal analysis, Investigation, Visualization, Data curation, Writing - review & editing, Project administration, Funding acquisition, Resources, Supervision.

Declaration of Competing Interest

The authors declare that they have no known competing financial interests or personal relationships that could have appeared to influence the work reported in this paper.

Acknowledgments

Cem Örnek is grateful for the financial support by TÜBİTAK (The Scientific and Technological Research Council of Turkey) under contract number 118C227 within the program “2232: International Fellowship for Outstanding Researchers”. Jinshan Pan and Fan Zhang are grateful for the financial support by Vinnova (Sweden’s innovation agency) under the contract number 2018-03267 within the program of “Industrial pilot projects for neutron and photon experiments at large scale research infrastructures.” Dirk L Engelberg and Robin Kroll are grateful for financial support by the Beijing Institute of Aeronautical Materials (China). Edvin Lundgren, Alfred Larsson, and Gary Harlow acknowledge the Swedish Research Council for financial support within the program Röntgen-Ångström Cluster “In-situ High Energy X-ray Diffraction from Electrochemical Interfaces (HEXCHEM)” under the project no. 2015-06092. Edvin Lundgren, Alfred Larsson, and Gary Harlow further express their gratitude for the support from the Nanometer Structure Consortium at Lund University (nmC@LU). All authors acknowledge Diamond Light Source for time on beamline I07 under proposal SI23388. The authors are grateful for Dr Ki-Hwan Hwang, KTH Royal Institute of Technology, and Lars Hässler, KTH Royal Institute of Technology, for designing and 3D-printing the electrochemical cell that was used in this work. The authors are also grateful for Prof Philip Withers, University of Manchester, for valuable feedback to the research proposal for synchrotron radiation time. Dr Timo Müller, Anton Paar GmbH, is acknowledged for helpful comments made on the work reported in this manuscript.

Appendix A. Supplementary data

Supplementary material related to this article can be found, in the online version, at doi:https://doi.org/10.1016/j.corsci.2020.109021.

References

[1] U. Kivisäkk, Relation of room temperature creep and microhardness to microstructure and HISC, Mater. Sci. Eng. A 527 (2010) 7684–7688.
[2] G. Chai, S. Ronneteg, U. Kivisäkk, R.L. Peng, S. Johansson, Mechanisms of hydrogen induced stress crack initiation and propagation in super duplex stainless steels, Steel Res. Int. 80 (2009) 482–487.
[3] M.S. Hazarabedian, A. Viereckl, Z. Quadir, G. Leadbeater, V. Golovanevskiy, S. Erdal, P. Georgeson, M. Iannuzzi, Hydrogen-induced stress cracking of swaged super duplex stainless steel subsea components, Corrosion 75 (2019) 824–838.
[4] G. Byrne, R. Francis, G. Warburton, Hydrogen induced stress cracking (HISC) resistance and improvement methods for super duplex stainless steels - paper No. 6981. Corrosion 2016, NACE International, Vancouver, British Columbia, Canada, 2016.
[5] M. Aursand, L.A. Marken, G. Rørvik, I.M. Kulbotten, Experiences with hydrogen induced stress cracking of duplex stainless steel components in subsea service with cathodic protection. Corrosion 2013, NACE International, Orlando, Florida, 2013, p. 15.
[6] C. Örnek, P. Reccagni, U. Kivisäkk, E. Bettini, D.L. Engelberg, J. Pan, Hydrogen embrittlement of super duplex stainless steel – towards understanding the effects of microstructure and strain, Int. J. Hydrogen Energy 43 (2018) 12543–12555.
[7] H.K.D.H. Bhadeshia, Prevention of hydrogen embrittlement in steels, Isij Int. 56 (2016) 24–36.
[8] O. Barrera, D. Bombac, Y. Chen, T.D. Daff, E. Galindo-Nava, P. Gong, D. Haley, R. Horton, I. Katzarov, J.R. Kermode, C. Liverani, M. Stopher, F. Sweeney, Understanding and mitigating hydrogen embrittlement of steels: a review of experimental, modelling and design progress from atomistic to continuum, J. Mater. Sci. 53 (2018) 6251–6290.
[9] M. Koyama, M. Rohwerder, C.C. Tasan, A. Bashir, E. Akiyama, K. Takai, D. Raabe, K. Tsuzaki, Recent progress in microstructural hydrogen mapping in steels: quantification, kinetic analysis, and multi-scale characterisation, Mater. Sci. Technol. 33 (2017) 1481–1496.
[10] R. Kirchheim, A. Pundt, 25 - Hydrogen in metals, in: D.E. Laughlin, K. Hono (Eds.), Physical Metallurgy, Fifth Edition, Elsevier, Oxford, 2014, pp. 2597–2705.
[11] C. Örnek, C. Leygraf, J. Pan, Passive film characterisation of duplex stainless steel using scanning Kelvin probe force microscopy in combination with electrochemical measurements, Npj Mater. Degrad. 3 (2019) 8.
[12] C. Örnek, A. Larsson, G. Harlow, F. Zhang, R. Kroll, F. Carlà, H. Hussain, U. Kivisäkk, D.L. Engelberg, E. Lundgren, J. Pan, Time-resolved grazing-incidence X-ray diffraction measurement to understand the effect of hydrogen on surface strain development in super duplex stainless steel, Scr. Mater. (2020).
[13] C. Örnek, T. Müller, U. Kivisäkk, F. Zhang, M. Långberg, U. Lienert, K.-H. Hwang, E. Lundgren, J. Pan, Operando time- and space-resolved high-energy X-ray diffraction measurement to understand hydrogen-microstructure interactions in duplex stainless steel, Corros. Sci. 175 (2020), 108899.
[14] T. Mente, T. Boellinghaus, Mesoscale modeling of hydrogen-assisted cracking in duplex stainless steels, Weld World 58 (2014) 205–216.
[15] D. Carrouge, H.K.D.H. Bhadeshia, P. Woollin, Effect of δ-ferrite on impact properties of supermartensitic stainless steel heat affected zones, Sci. Technol. Weld. Join. 9 (2004) 377–389.
[16] U. Welzel, J. Ligot, P. Lamparter, A.C. Vermeulen, E.J. Mittemeijer, Stress analysis of polycrystalline thin films and surface regions by X-ray diffraction, J. Appl. Crystallogr. 38 (2005) 1–29.
[17] T. Mente, T. Bollinghaus, Modeling of hydrogen distribution in a duplex stainless steel, Weld World 56 (2012) 66–78.
[18] C.M. Schlepütz, S.O. Mariager, S.A. Pauli, R. Feidenhans’l, P.R. Willmott, Angle calculations for a (2+3)-type diffractometer: focus on area detectors, J. Appl. Crystallogr. 44 (2011) 73–83.
[19] C. Örnek, A. Larsson, G.S. Harlow, F. Zhang, R. Kroll, F. Carlà, H. Hussain, U. Kivisäkk, D.L. Engelberg, E. Lundgren, J. Pan, Time-resolved grazing-incidence X-ray diffraction measurement to understand the effect of hydrogen on surface strain development in super duplex stainless steel, Scr. Mater. 187 (2020) 63–67.
[20] E.S. Statnik, A.I. Salimon, F. Uzun, A.M. Korsunsky, Polar transformation of 2D X-ray diffraction patterns for 2D strain evaluation, in: S.I. Ao, L. Gelman, D. W. Hukins, A. Hunter, A.M. Korsunsky (Eds.), The World Congress on Engineering 2019, WCE, London, 2019, pp. 397–401.
[21] K. Knipe, A. Manero, S.F. Siddiqui, C. Meid, J. Wischek, J. Okasinski, J. Almer, A. M. Karlsson, M. Bartsch, S. Raghavan, Strain response of thermal barrier coatings captured under extreme engine environments through synchrotron X-ray diffraction, Nat. Commun. 5 (2014) 4559.
[22] O. Takakuwa, Y. Mano, H. Soyama, Effect of hydrogen on the Micro- and macro-strain near the surface of austenitic stainless steel, Adv. Mat. Res. 936 (2014) 1298–1302.
[23] L.C.D. Fielding, E.J. Song, D.K. Han, H.K.D.H. Bhadeshia, D.-W. Suh, Hydrogen diffusion and the percolation of austenite in nanostructured bainitic steel, Proc. R. Soc. A 470 (2014) 18.
[24] C. Örnek, P. Reccagni, U. Kivisäkk, E. Bettini, D.L. Engelberg, J. Pan, Hydrogen embrittlement of super duplex stainless steel – towards understanding the effects of microstructure and strain, Int. J. Hydrogen Energy 43 (2018) 12543–12555.

[25] S. Chen, M. Gao, R.P. Wei, Hydride formation and decomposition in electrolytically charged metastable austenitic stainless steels, Metall. Mat. Trans. A 27 (1996) 29–40.
[26] K. Kamachi, An X-ray study of hydrides formed in austenitic stainless steels, Trans. Iron Steel Inst. Jpn. 18 (1978) 485–491.
[27] Y. Fukai, Site preference of interstitial hydrogen in metals, J. Less Common Met. 101 (1984) 1–16.
[28] Q. Yang, J.L. Luo, Martensite transformation and surface cracking of hydrogen charged and outgassed type 304 stainless steel, Mater. Sci. Eng. A 288 (2000) 75–83.
[29] Y. Tian, S. Lin, J.Y.P. Ko, U. Lienert, A. Borgenstam, P. Hedström, Micromechanics and microstructure evolution during in situ uniaxial tensile loading of TRIP-assisted duplex stainless steels, Mater. Sci. Eng. A 734 (2018) 281–290.
[30] J.J. Hoyos, E.A. Torres, J.R. Fernández, P. Craidy, M.T.P. Paes, A.J. Ramírez, A. P. Tschiptschin, In situ synchrotron radiation measurements during axial strain in hydrogen cathodically charged duplex stainless steel SAF 2205, Mater. Res. 21 (2018).
[31] O. Takakuwa, Y. Mano, H. Soyama, Increase in the local yield stress near surface of austenitic stainless steel due to invasion by hydrogen, Int. J. Hydrogen Energy 39 (2014) 6095–6103.
[32] D.N.V. (DNV), Recommended Practice DNV-RP-F112 Design of Duplex Stainless Steel Subsea Equipment Exposed to Cathodic Protection, Det Norkse Veritas, Norway, 2008.
[33] M. Iannuzzi, 15 - Environmentally assisted cracking (EAC) in oil and gas production, in: V.S. Raja, T. Shoji (Eds.), Stress Corrosion Cracking, Woodhead Publishing, 2011, pp. 570–607.
[34] R. Francis, Stress Corrosion Cracking of Duplex Stainless Steels, MTI, 2014, p. 58.
[35] K. Nakade, T. Kuroda, The fracture analysis for hydrogen embrittlement of super duplex stainless steel weld metal, J. Soc. Mater. Sci. Jpn. 54 (2005) 215–220.
[36] K. Toshio, N. Katsuyuki, Behavior of Hydrogen in Super Duplex Stainless Steels, 37, Transactions of Joining and Welding Research Institute, 2008.